CoA. Note Aero 158

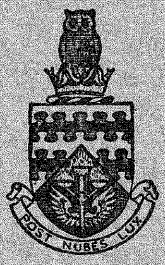

THE COLLEGE OF AERONAUTICS
CRANFIELD

AN INVESTIGATION OF VORTEX BREAKDOWN AT MACH 2

by

A. H. Craven and A. J. Alexander

CoA Note Aero 158

November, 1963

THE COLLEGE OF AERONAUTICS

DEPARTMENT OF AERODYNAMICS

An investigation of vortex breakdown at Mach 2

- by -

Squadron Leader A.H. Craven, M.Sc., Ph.D., D.C.Ae., A.F.R.Ae.S.

and

A.J. Alexander, M.Sc., Ph.D., A.F.R.Ae.S.

SUMMARY

Wind tunnel tests have been made at M = 2 on a 75° swept delta wing in order to study the progressive breakdown of the leading edge vortices, which occurs at high incidence. The incidence at which vortex breakdown occurred at supersonic speeds was somewhat less than at low speeds, but the pattern of breakdown appeared to be similar, although the spiralling region of flow is much larger at supersonic speeds.

Quite slender objects placed downstream of the wing had appreciable upstream effects, causing vortex breakdown to move upstream by as much as 20% of the root chord for the same incidence.

Contents

List of symbols

α	geometric incidence
C_o	root chord
s	wing semi-span
M_o	free stream Mach number
x, y	chordwise and spanwise distances
p	surface static pressure
p_o	free stream static pressure
C_p	pressure coefficient $= \frac{p - p_o}{\frac{1}{2}\rho V^2} = \frac{\frac{p}{p_o} - 1}{\frac{\gamma}{2} M^2}$

1. Introduction

The breakdown of the leading edge vortices generated by highly swept wings at moderate and high incidence has been studied by several authors (ref. 1 - 4). Most of the experimental work has been performed either in low speed wind tunnels, or at very low speeds in water tunnels. Substantial agreement is obtained over a wide range of speeds, and it is generally accepted that the Reynolds number effect is small.

Vortex breakdown is thought to be due to an adverse axial pressure gradient along the vortex core, causing stagnation of the axial flows followed by a spiralling motion round a region of slowly moving fluid. Downstream of this region there is a breakdown into large scale turbulence. In tests at high subsonic speed, by Lambourne and Bryer[1], the flow appears to have three distinct regions, as in incompressible flow. Schlieren pictures show the tightly coiled vortex from the apex which thickens immediately downstream of a normal shock, breakdown to large scale turbulence occurring downstream of the trailing edge shock. It is not possible to detect any spiralling motion in the middle region, although there is no reason to suppose that it does not exist. In tests by Elle[4], similar pictures are obtained, although the vortex breakdown referred to in that paper would appear to correspond to the beginning of the middle region in Lambourne and Bryer's description, and not to the final breakdown to large scale turbulence.

Tests made by Edney and Stevenson[5] to investigate vortex breakdown at supersonic speed on 75° delta wings showed that vortex breakdown occurred at much lower incidences ($\approx 17°$) than would be expected from results obtained at low speeds. However, tests at the Royal Aircraft Establishment and the Aircraft Research Association[6] on wings and wing-body combinations with similar angles of sweep suggested that vortex breakdown did not occur over the wing at incidences below 25°. It was therefore inferred that the vortex breakdown obtained by Edney and Stevenson was due to some form of wind tunnel interference. Scale effect was discounted as their tests had been performed at various tunnel stagnation pressures and with models whose root chord varied from 5 to 8 inches, giving a range of Reynolds numbers between 5.75×10^5 and 12.8×10^5 in which the reference length was the root chord of the model.

The tests described in this report were undertaken to resolve this anomaly and to obtain a more comprehensive understanding of the phenomenon.

2. The model and the experimental method

The model was a 75° swept delta wing of 5 in. root chord with a flat upper surface and bevelled lower surface, giving a sharp leading edge having an included angle of 16°. The model was sting mounted on a half quadrant, so that no part of the mounting protruded above the plane of the model (fig. 1). The arrangement of the static pressure holes is shown in fig. 2 and comprised a spanwise row of 9 holes at 79% root chord, and a row of 6 holes in the range 0.4 - 0.9 c_o, at 60% semi-span along a

ray through the apex.

The Schlieren photographs were taken using a spark discharge. In most of the photographs the knife edge of the Schlieren system was horizontal, but a few photographs were taken with the knife edges vertical to obtain better definition in some parts of the breakdown region.

The tests were made in the College of Aeronautics 9" × 9" supersonic tunnel, at a Mach number of 1.96 with a stagnation pressure of 5 lb/sq.in. absolute, giving a Reynolds number of 5.75×10^5 based on the root chord length of the model.

3. Discussion of results

Results were obtained in the incidence range 13° - 34° and included static pressure measurements along a line at 79% root chord and along a line through the apex at 69% semi-span. From the Schlieren photographs, figs. 3a and 3b have been compiled. At low incidences (≈ 10°) some thickening of the vortex core is observed downstream of the trailing edge, but no evidence of spiralling could be seen in the field of view which extended 1½ chord lengths downstream of the trailing edge. At higher incidence (≈ 25°) three distinct flow regions could be seen.

(i) The tightly rolled core, followed by

(ii) a region of spiralling flow bounded upstream by a conical shock, and finally

(iii) breakdown to large scale turbulence.

This is sketched in fig. 3a and is similar to conditions observed at low speeds, except that the streamwise extent of the spiralling region is much larger at supersonic speeds. Fig. 3b shows the observed shock pattern at the higher incidence.

Figure 4a (α = 13°) shows the thickening of the core downstream of the trailing edge shock, with no breakdown into turbulence. At α = 18° (fig. 4b), however, there is definite evidence of spiralling behind the trailing edge shock and a second almost horizontal shock originates at the trailing edge (shock 2 in fig. 3b). The formation of shock 1 will depend on the angle through which the flow is required to turn on approaching the upper surface and has apparently not formed at α = 18°. At α = 23°, both shocks are clearly visible interacting downstream of the trailing edge, both being deflected. Downstream of the interaction, shock 1 weakens and fades as it approaches the wake, and its function of turning the swirling flow is taken over by shock 2. At α = 26°, breakdown of the vortex flow to large scale turbulence can be seen to the right of the photograph. This coincides with the disappearance of the trailing shock (shock 2), indicating much lower swirling velocities in that region, as would be expected. Although it is not clear from the

photograph, it is probable that, at this incidence (26°), the change from a tightly rolled vortex to the spiralling motion occurs just upstream of the trailing edge. In the range of incidence up to 26°, the trailing edge shock is strongest in the region above the vortices, where it must turn the entire flow. Nearer the wing it is more normal to the wing surface and appears to be weaker since it is restricted to a small region between the vortices.

When the incidence has reached 30°, the initial change to a spiralling motion occurs at 80% of the root chord and small shock waves can be seen at the upstream boundary. These shock waves bounding the spiral motion were definitely unsteady around this incidence. Although the lower part of the conical shock upstream of the spiralling region cannot be seen in these photographs, its existence is established in reference 5. Its position in these tests can be inferred from its visible upper part and coincides with the change in direction of shock 1 at about 85% chord. The horizontal shock at the trailing edge is now shorter, but its disappearance still coincides with the final breakdown to turbulence.

At $\alpha = 31°$, the three regions of breakdown can be clearly seen. The change to spiralling motion occurs at about 60% chord and is bounded by a conical shock. Shock 1 close to the surface is turned and weakened by the conical shock at about 80% chord. This is confirmed by a pressure rise (Fig. 7). The change in direction of shock 1 indicates that the flow near the surface is turned towards the main-stream direction, thus reducing the angle through which it must be turned by shock 2. In addition, because of the thickening, the vortices have moved further from the surface and hence the downward component of the swirling velocity near the plane of the wing downstream of the trailing edge is reduced. For these reasons there is little turning action required of shock 2. It appears as a very weak shock extending only a small distance from the trailing edge. Breakdown to turbulence occurs at about 20% chord downstream of the trailing edge. The trailing edge shock is now quite weak and indistinct. It does not appear to penetrate between the vortices.

As the incidence is further increased, the change to spiralling flow moves forward until, at $\alpha = 34°$, it occurs at about $^1/_3$ root chord and coincides with the disappearance of shock 1. The onset of the surface pressure rise also moves forward. At $\alpha = 34°$, the pressure is affected at least as far forward as 50% root chord (fig. 7).

Since the upstream influence of the quadrant used in the previous tests in this tunnel appeared to be so large, it was decided to find the effect of various objects placed downstream of the model. Although the cause of this considerable upstream influence has not been determined, it was felt that it may have an important effect on, say, missiles with delta canard control surfaces, the main wing forming an obstruction downstream. The first tests were made with a 'fin' approximately 6 in. long and 1 in. chord, having a double wedge section 0.2 in. thick, mounted on the sling at the position of the old quadrant mounting. This 'fin' was considerably

smaller than the original quadrant. Unfortunately, the effective height of the 'fin' decreased as the incidence was decreased, owing to the rotation of the half-quadrant mounting but at $\alpha = 17°$ (where vortex breakdown suddenly occurred on the wing with the full quadrant mounting) the top of the fin was still well above the tunnel centre line. However, no effect whatsoever was apparent with the 'fin' in this position, the pressures and Schlieren photographs being identical with those obtained with the plain wing.

Figures 8a and 8b show the 'fin' mounted at 70% downstream of the trailing edge, at incidences of 26° and 30°. Comparison with figures 4d and 6a shows that the whole flow pattern has been moved upstream some 20% of the chord. The effect is also visible in the pressure distributions (fig. 10).

Figures 9a and 9b, also taken at $\alpha = 26°$ and 30° respectively, show the effect of a smaller 'fin' just behind the trailing edge. Comparison with figures 8a and 8b shows that the change to spiralling motion is hardly affected although, at $\alpha = 30°$ at least, breakdown to turbulence occurs further upstream.

4. Suggestions for further work

The tests described in this report have clarified some of the points raised in the earlier work, but much remains to be done. More tests are proposed with the existing models and equipment as follows.

(1) More comprehensive pressure plotting to find the effect of vortex breakdown on the upper surface lifts.

(2) Surface flow visualisation.

(3) Detailed exploration of the flow using high speed ciné photography.

(4) Tests with more representative objects (e.g. fins) downstream of the model to find their effect on vortex breakdown.

(5) Tests with a cylindrical body and ogival noses of various lengths.

5. Conclusions

Tests on a 75° swept delta wing at $M \approx 2$ have shown the existence of vortex breakdown at incidences only slightly less than those at which breakdown occurs at low speeds. The breakdown follows a pattern similar to that found at low speeds. A tightly rolled vortex is followed by an extended region in which the vortex has thickened and is probably spiralling. This region ultimately degenerates into the final breakdown to large scale turbulence. The main difference from the breakdown at low speeds appears to be that the middle (spiralling) region occupies a much larger area at supersonic speeds (of the order of a chord length). At low speeds it

occupies only a fraction of the chord, and it is not always possible to distinguish it from the final breakdown to turbulence, the two regions together being loosely described as 'vortex breakdown'.

The presence of an object downstream of the wing, with its associated shock system, can cause vortex breakdown to occur further upstream. The way in which this disturbance is propogated upstream is not known, but it could well have undesirable effects when canard control surfaces are used in either aircraft or missiles, when the wing could act as a downstream obstruction.

6. Acknowledgment

The authors are indebted to Mr. S.H. Lilley for his considerable assistance with the wind tunnel tests.

7. References

1. Lambourne, N.C. and Bryer, D.N. — The bursting of leading edge vortices - some observations and discussion of the phenomenon. A.R.C. R. and M. 3282, 1962. ARC 22775

2. Werlé, H. — Sur l'eclatements des tourbillons d'apex d'une aile delta aux faibles vitesse. Rech. Aero., No. 74, 1960, pp. 23-30.

3. Jones, J.P. — The breakdown of vortices in separated flow. U.S.A.A. Rept. 140. A.R.C. 22241, 1960.

4. Elle, B.J. — On the breakdown at high incidences of the leading edge vortices on delta wings. J. Roy. Aero. Soc., Vol. 64, 1960, p. 49.

5. Edney, B.E. and Stevenson, Mrs. M.A. — Vortex breakdown at Mach 2. College of Aeronautics unpublished thesis. 1963.

6. - — Private communication.

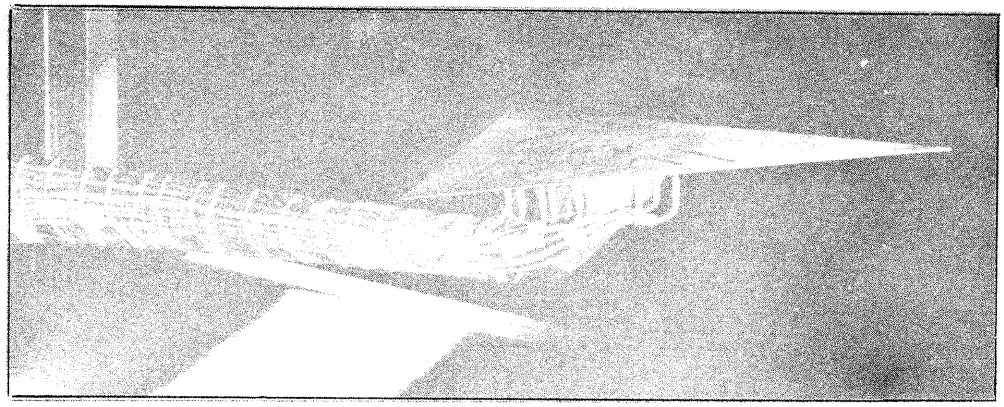

FIG. 1 MODEL MOUNTED IN TUNNEL

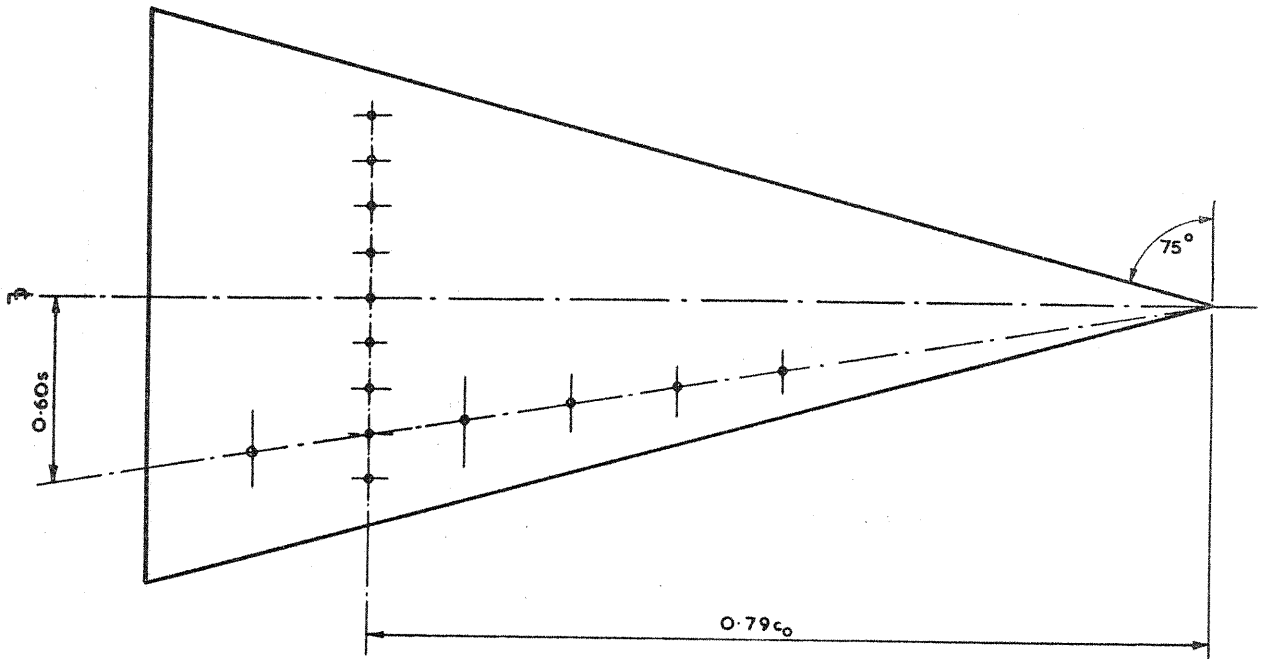

FIG. 2 THE POSITION OF THE PRESSURE TAPPINGS

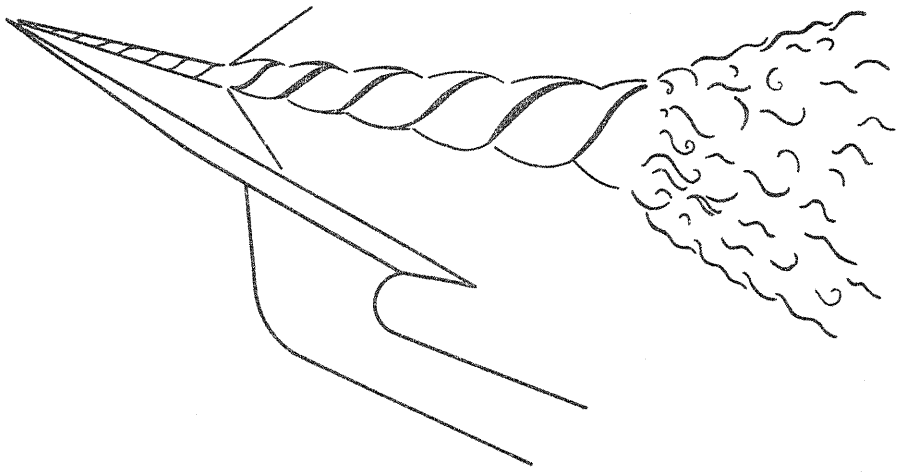

FIG. 3a THE PROCESS OF BREAKDOWN AT SUPERSONIC SPEEDS $\alpha \approx 30°$

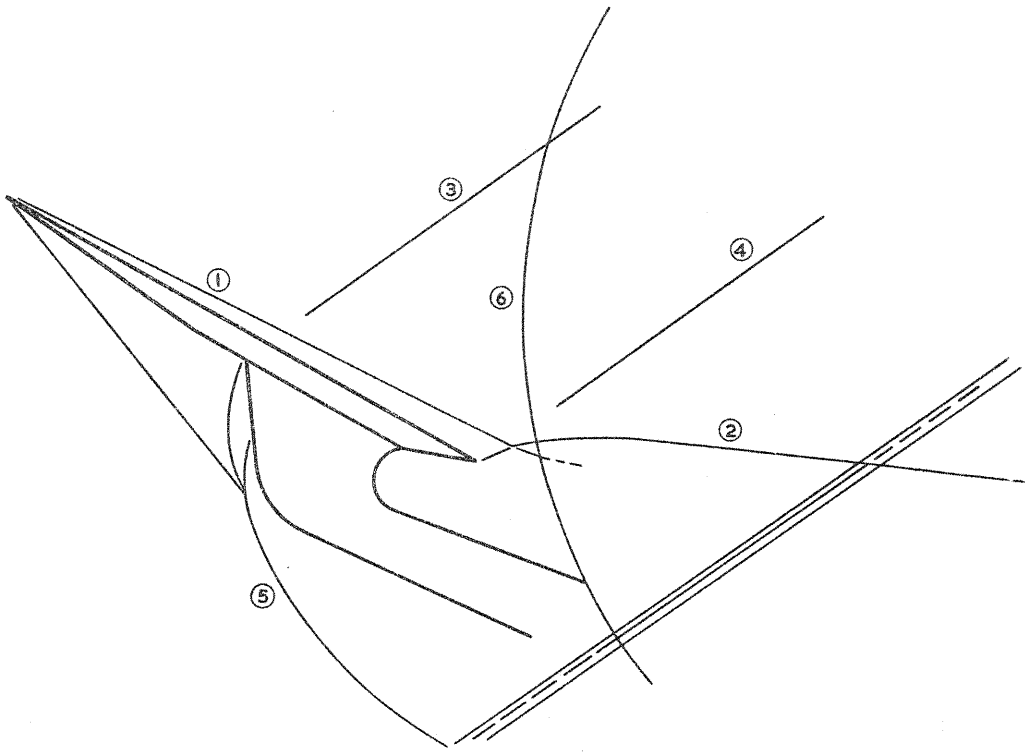

FIG. 3b SHOCK WAVE PATTERN

(1) Shock wave close to surface associated with turning of downward swirling flow to free stream direction.

(2) Shock wave springing from trailing edge associated with turning of flow parallel to the surface at the trailing edge to new mainstream direction
Interaction of (1) and (2) deflects both shocks.

(3) Mach wave caused by disturbance at leading edge of undersurface shock from mounting.

(4) Trailing edge shock. Only visible above vortices at high incidence.

(5) Complex shock system comprising bow shock and shocks from mounting.

(6) Reflection of (5) on tunnel window.

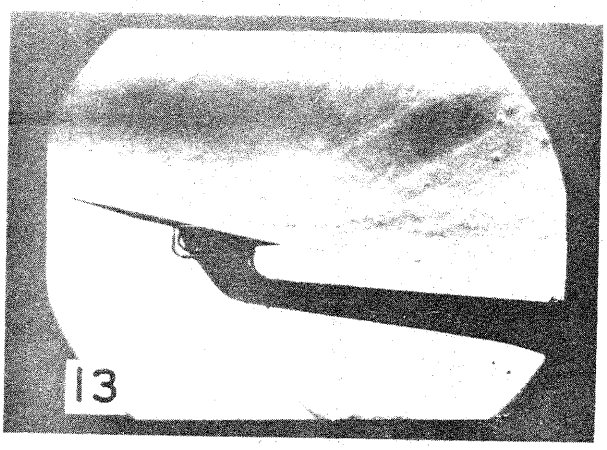

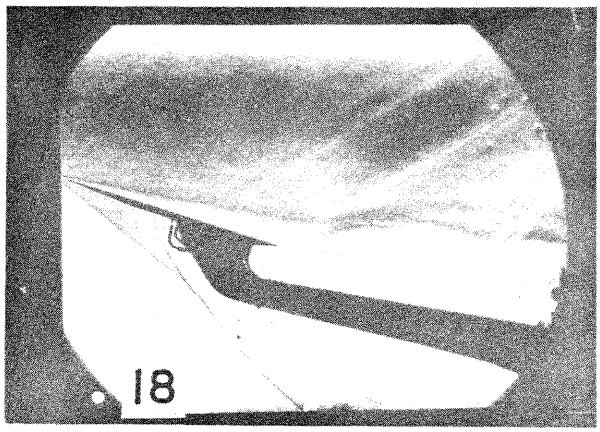

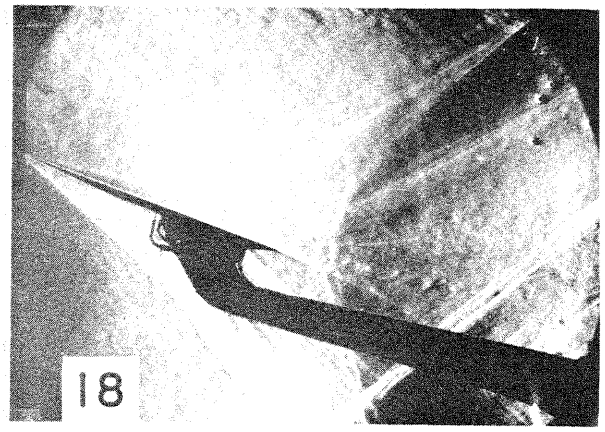

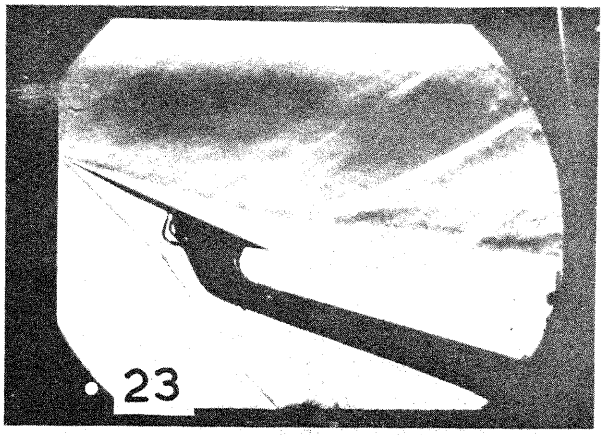

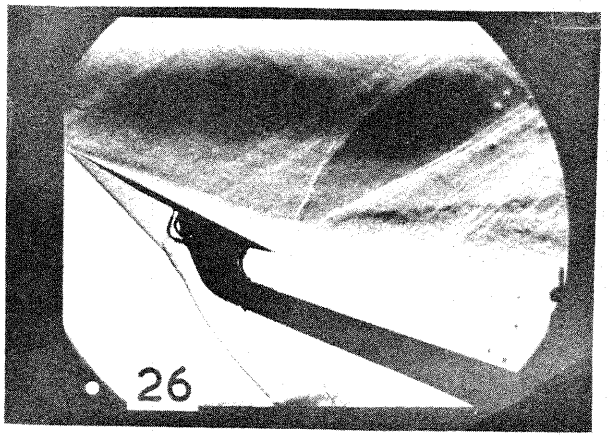

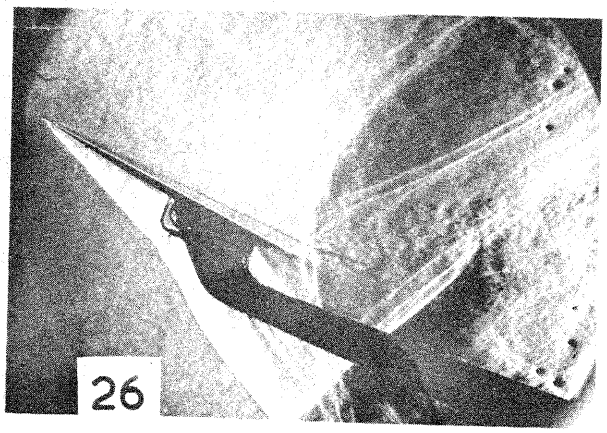

FIGS. 4a to 4d SCHLIEREN PHOTOGRAPHS WITH PLAIN MODEL $\alpha = 13^{\circ} - 26^{\circ}$

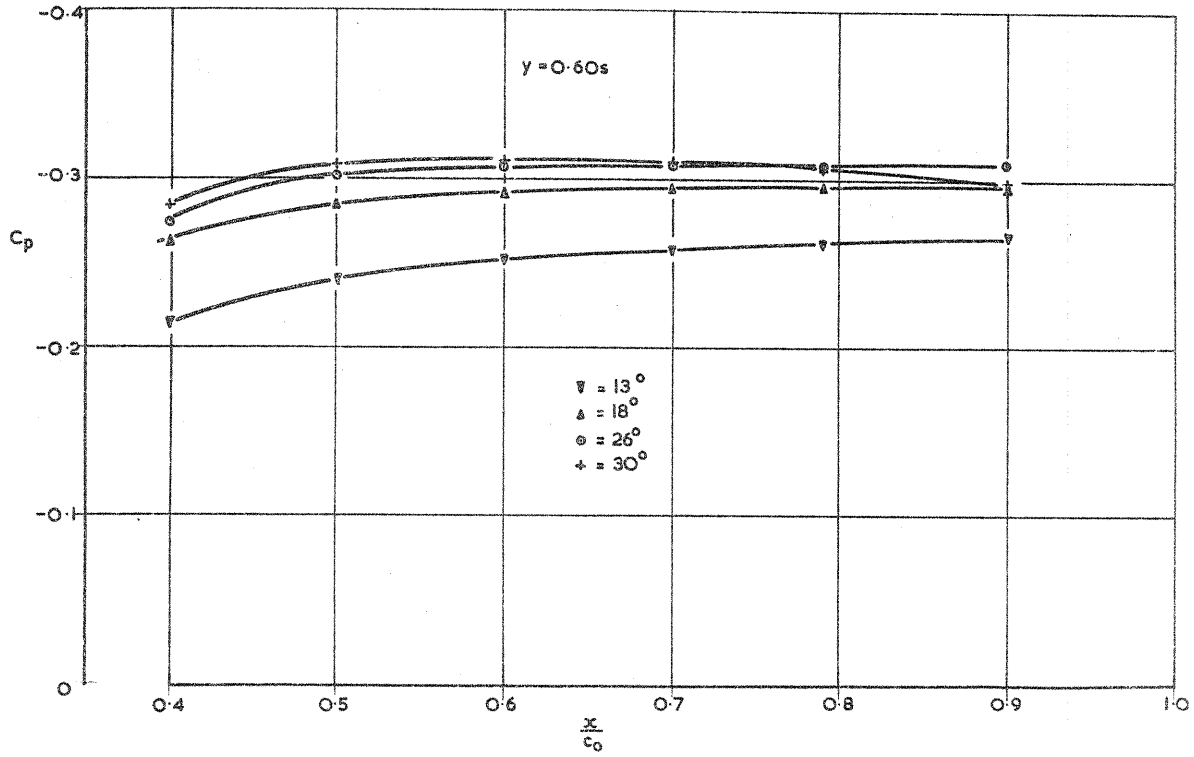

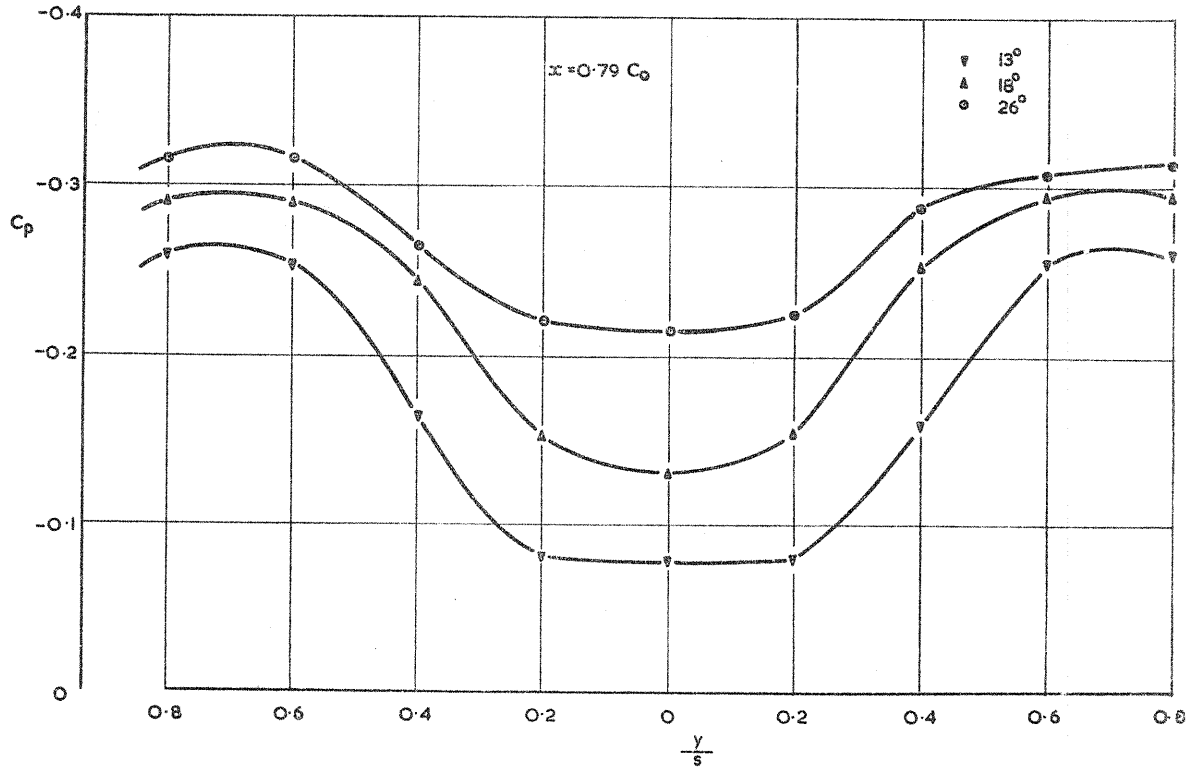

FIG. 5 STATIC PRESSURE DISTRIBUTIONS AT 0.6 SEMI-SPAN AND 0.79 ROOT CHORD. PLAIN WING.

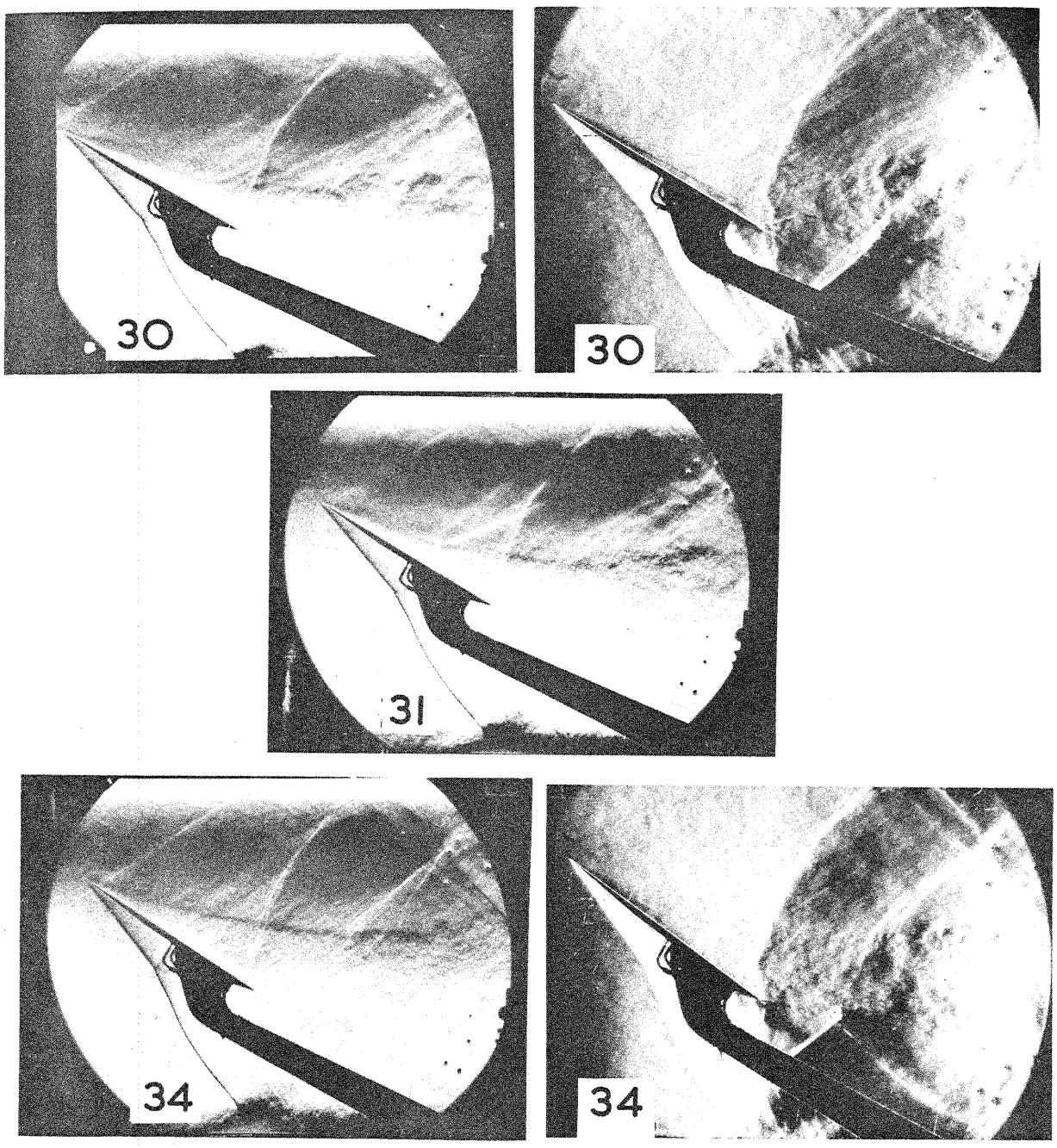

FIGS. 6a to 6c SCHLIEREN PHOTOGRAPHS WITH PLAIN MODEL $\alpha = 30^{\circ} - 34^{\circ}$

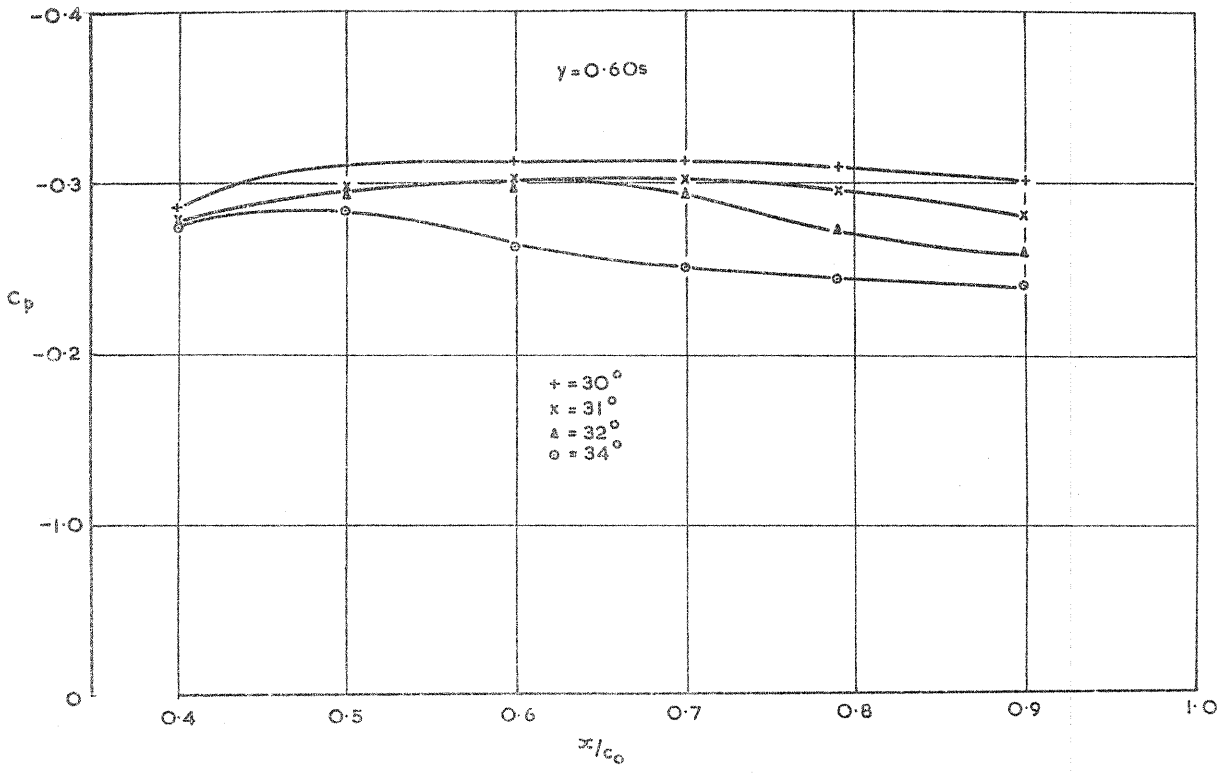

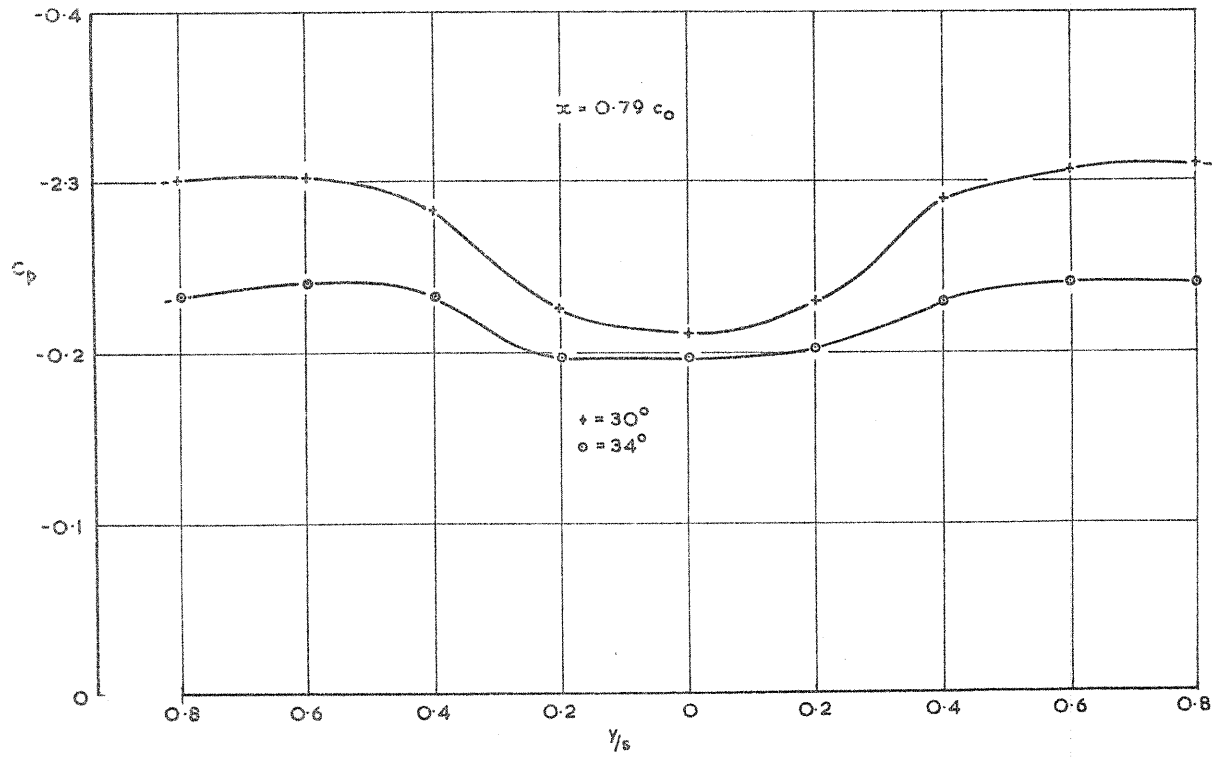

FIG. 7 STATIC PRESSURE DISTRIBUTIONS AT 0.6 SEMI-SPAN AND 0.79 ROOT CHORD. PLAIN WING.

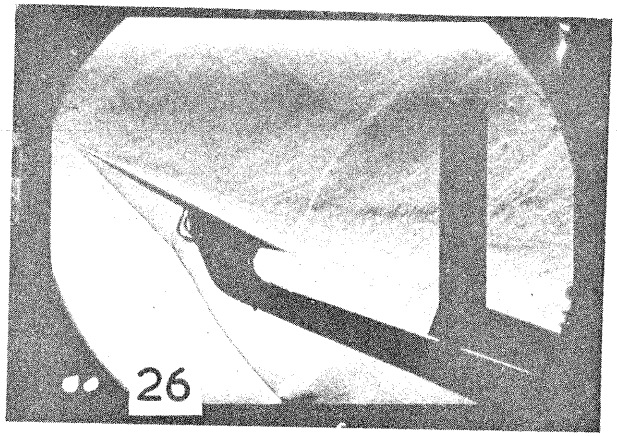

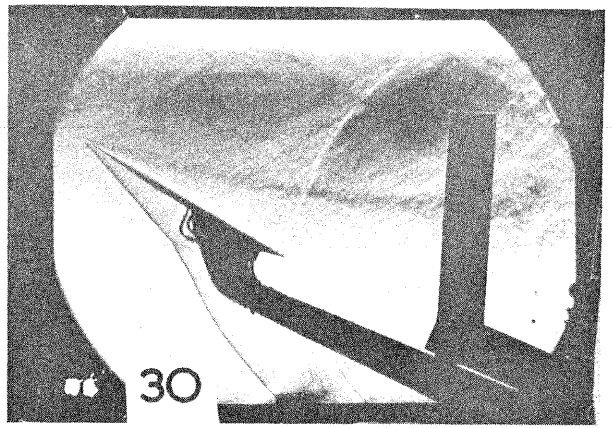

FIG. 8a and 8b SCHLEIREN PHOTOGRAPHS WITH LARGE 'FIN' 0.7c_o DOWNSTREAM OF TRAILING EDGE.

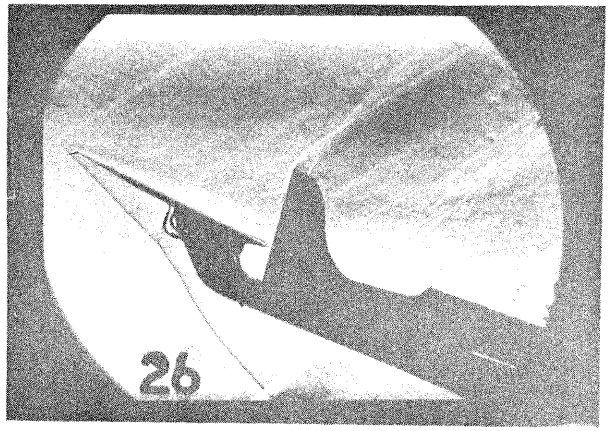

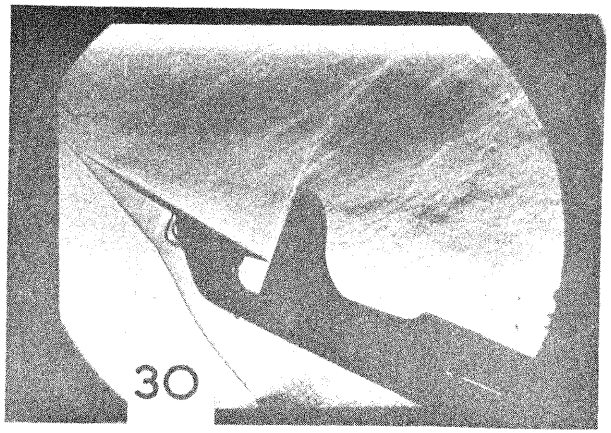

FIG. 9a and 9b SCHLIEREN PHOTOGRAPHS WITH SMALL FIN AT TRAILING EDGE

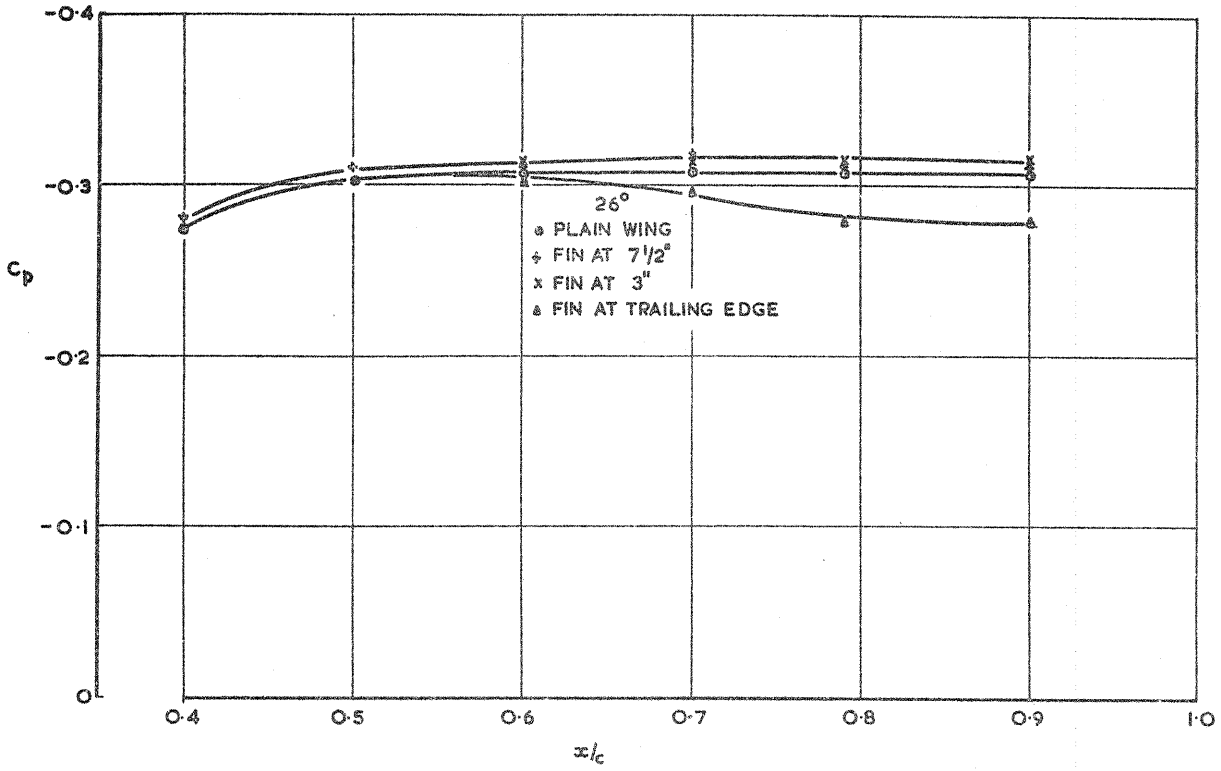

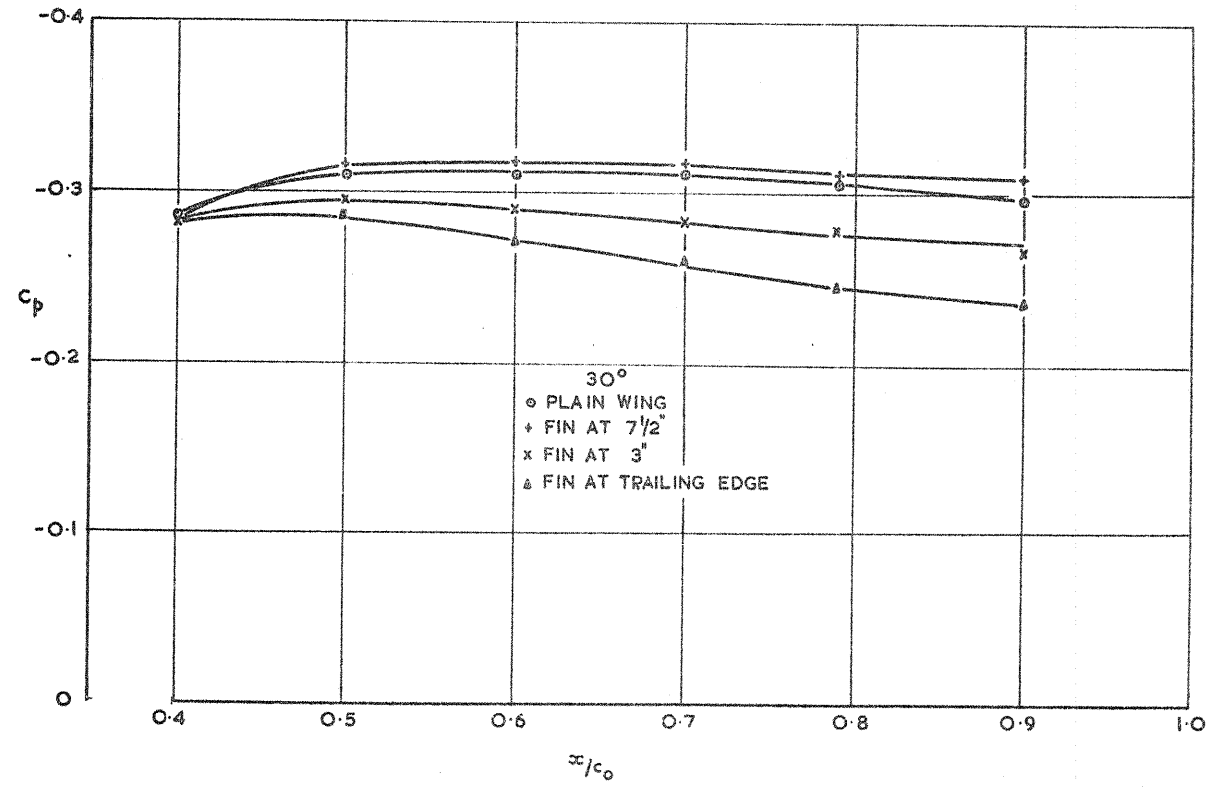

FIG. 10 EFFECT OF 'FINS' ON STATIC PRESSURE DISTRIBUTION AT 0.6 SEMI-SPAN.